J Mater Sci: Mater Electron (2009) 20:177–180
DOI 10.1007/s10854-008-9678-1

AFM fabrication and characterization of nanoscale Al_2O_3 patterns

Zheng Jiao · Haijiao Zhang · Minghong Wu · Huijiao Guo · Jia Wang · Bing Zhao · Guoji Ding

Received: 23 November 2007 / Accepted: 26 February 2008 / Published online: 24 March 2008

Abstract In this paper the atomic force microscopy (AFM) fabrication of nanoscale Al_2O_3 patterns were studied. Nanowire, rings, dot array and pattern were fabricated on Si substrates with SiO_2 surface layer. The effects of applied voltage and scanning speed on obtained Al_2O_3 pattern were evaluated and the anodic oxidation mechanism was discussed.

1 Introduction

The use of a scanning tunneling microscopy (STM) or an atomic force microscopy (AFM) has become a powerful technique for the fabrication of semiconductor nanoscale structures. Many related works have been reported since Dagata et al. [1] presented the STM direct writing oxidation process using the oxide as a mask for a pattern transfer. STM based anodic oxidation on metallic substrates such as Ti has been also reported [2–4]. AFM was also adopted to generate oxide patterns on Ti [5–9].

In this paper we report the oxide patterning on Al thin film surface using contact mode AFM in ambient atmosphere. Nanowire, rings, dot array and pattern were fabricated. The effects of applied voltage and scanning speed on obtained Al_2O_3 pattern were evaluated and the anodic oxidation mechanism was discussed.

Z. Jiao · M. Wu (✉)
School of Environmental & Chemical Engineering,
Shanghai University,
Shanghai 201800, China
e-mail: mhwu@staff.shu.edu.cn

Z. Jiao
e-mail: zjiao@shu.edu.cn

H. Zhang · H. Guo · J. Wang · B. Zhao · G. Ding (✉)
Institute of Nanochemistry and Nanobiology,
Shanghai University, Shanghai 201800, China
e-mail: gjding@shu.edu.cn

2 Experimental

The p-type Si(100) wafers were used as substrates. First they were cleaned by standard RCA procedure, then grown a 0.3 μm thick SiO_2 surface layer. A 12 nm thick Al layer were sputtered on the Si substrates with a deposition rate of 0.1 nm/s. The specimen were glued onto the holder by silver paste, then placed in a SEIKO's SPI3700/SPA300 AFM, which provide anodic oxidation functions. The AFM worked in contact mode and relative humidity was 60%. The cantilevers were Au coated Si_3N_4 tips available from Olympus company. The nanoscale Al_2O_3 patterns' morphology were observed by the same AFM.

3 Results and discussion

Figure 1 shows AFM images of Al_2O_3 lines, rings, dot arrays, patterns, respectively. The results prove that AFM has good efficiency of oxidation on fabricating nanoscale Al_2O_3 patterns. All patterns are uniform and intact.

Figure 2 is the scheme of charge movements inside thin films in AFM anodic oxidation. J_i, J_e are the current caused by ion and electron, respectively. J is the whole current. X_0 is the thickness of oxide layer grown with the oxidation, X_i is the thickness of oxide layer before oxidation. f is the movement of anion, n_i is the concentration of anion in oxide layer.

In the oxide layer,

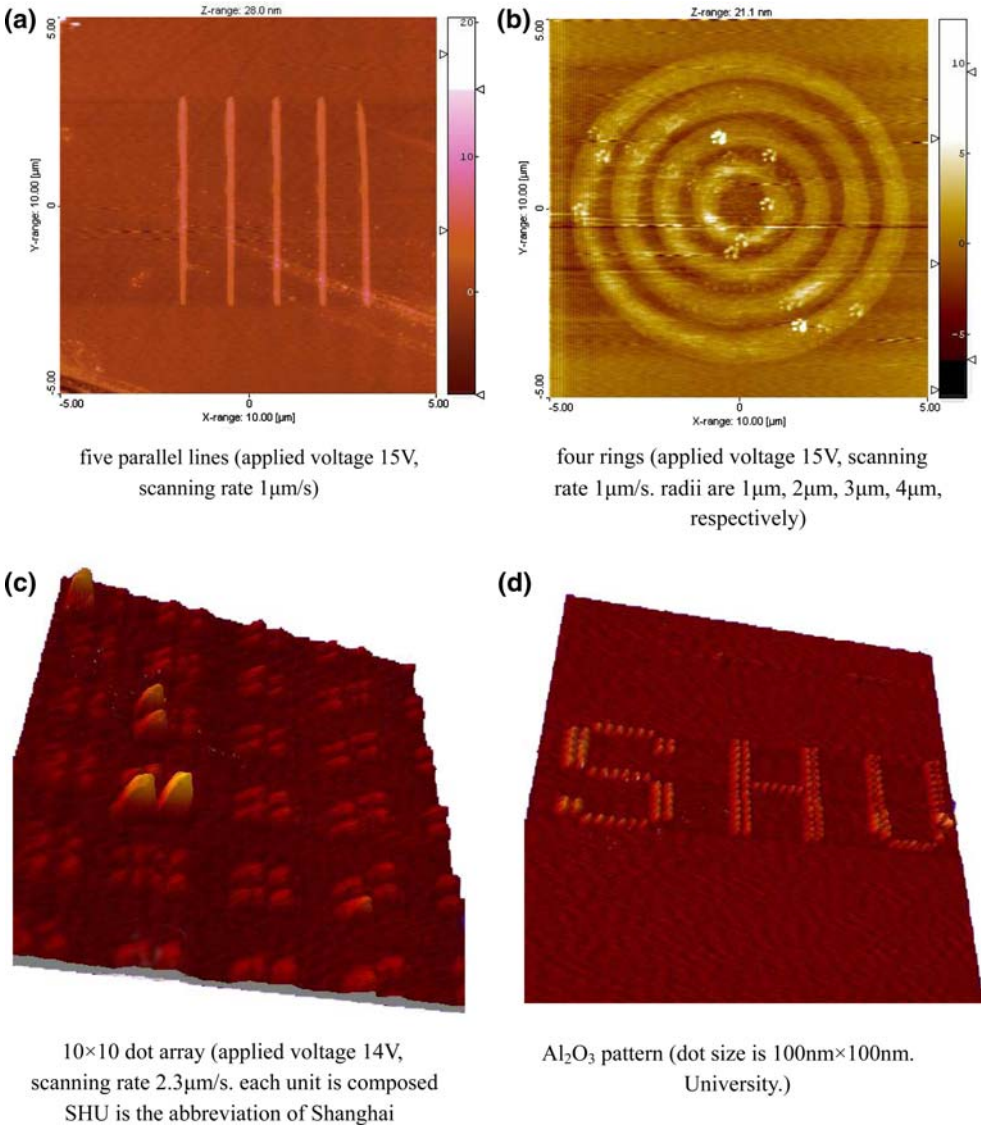

Fig. 1 AFM images of Al_2O_3 patterns generated by anodic oxidation. (**a**) Five parallel lines (applied voltage 15 V, scanning rate 1 µm/s), (**b**) four rings (applied voltage 15 V, scanning rate 1 µm/s. radii are 1, 2, 3 and 4 µm, respectively), (**c**) 10 × 10 dot array (applied voltage 14 V, scanning rate 2.3 µm/s. each unit is composed of a 2 × 2 array. The dot size is 70 × 70 nm), (**d**) Al_2O_3 pattern (dot size is 100 × 100 nm. SHU is the abbreviation of Shanghai University

$$J_i = -n_i q \mu_i E = -n_i q \mu_i \frac{V}{X_0(t)} \tag{1}$$

and

$$J_i = -qf \tag{2}$$

where μ_i is the rate of anion movement, E is the electric field inside the oxide layer, V is the applied voltage on oxide layer.

The current efficiency of ion η is,

$$\eta = \frac{J_i}{J} \tag{3}$$

$$J = J_i + J_e \tag{4}$$

The anion reached the Si interface is,

$$f = N_1 \frac{dX_0(t)}{dt} \tag{5}$$

It follows from formula (5) and formula (2),

$$J_i = -qN_1 \frac{dX_0(t)}{dt} \tag{6}$$

where N_i is the anion concentration in oxide layer.

The applied voltage on oxide layer is

$$V = V_0 - JAR \tag{7}$$

where R is the impendence of Si layer and A is the area of oxide layer.

It follows from formula (7) and formula (1),

$$J_i = -\frac{n_i q \mu_i}{X_0(t)}(V_0 - JAR) \tag{8}$$

Assume the slight changes in current efficiency of ion can be omitted, so

$$J \approx \frac{J_i}{\eta_{av}} \tag{9}$$

where

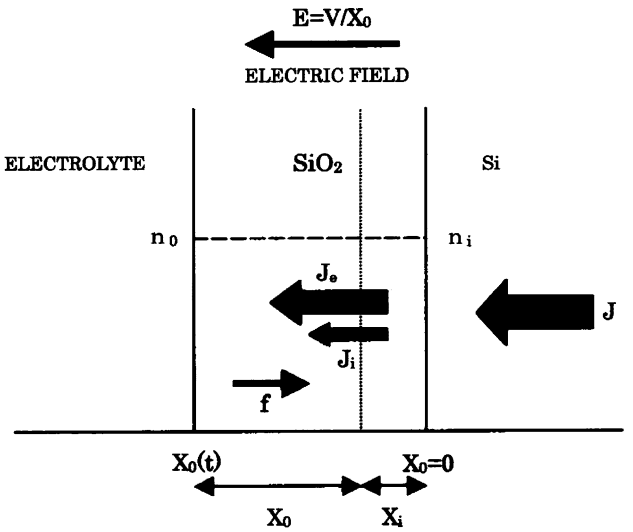

Fig. 2 The scheme of charge movements inside thin films in AFM anodic oxidation

$$\eta_{av} = \frac{1}{t_f - t_i}\int_{t_i}^{t_f} \eta(t)dt$$

It follows from formula (9) and formula (8),

$$J_i = -\frac{n_i q \mu_i V_0 \eta_{av}}{X_0 \eta_{av} - n_i q \mu_i AR} \tag{10}$$

follows from formula (10) and formula (5), we have

$$\frac{dX_0}{dt} = \frac{n_i q \mu_i V_0 \eta_{av}}{qN_1 \eta_{av} X_0(t) - n_i \mu_i q^2 N_1 AR} \tag{11}$$

For the boundary condition $t = 0$, $X_0(t) = 0$,

$$\int_0^t dt = \int_0^{X_0 - X_i} \left[\frac{qN_i X(t)}{n_i \mu_i V_0} - \frac{qN_i AR}{V_0 \eta_{av}}\right] dx \tag{12}$$

where X_i is the thickness of oxide layer before oxidation.

When $X_0 > 0$, Solve Eq. 12, we have

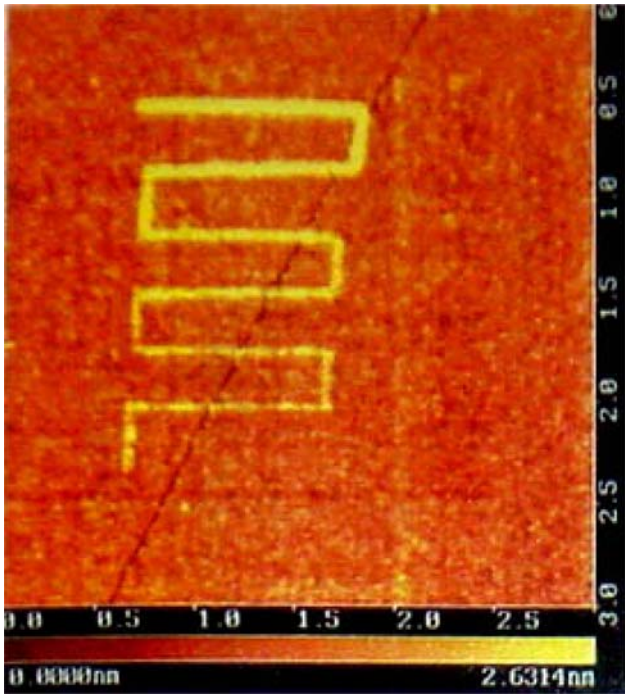

Fig. 4 The AFM fabricated Al_2O_3 lines under different scanning rates. (The applied voltage is 12 V. From above to bottom the scanning rates were 0.05, 0.1, 0.5, 1, 2 and 5 μm/s, respectively)

$$X_0 = \frac{n_i q \mu_i AR}{\eta_{av}} + \sqrt{\left(\frac{n_i q \mu_i AR}{\eta_{av}}\right)^2 - \left(\frac{2n_i \mu_i V_0}{N_i}\right)t} \tag{13}$$

Add X_i to formula (13), we have

$$X_0(t) = X_i + \frac{n_i q \mu_i AR}{\eta_{av}} + \sqrt{\left(\frac{n_i q \mu_i AR}{\eta_{av}}\right)^2 - \left(\frac{2n_i \mu_i V_0}{N_i}\right)t} \tag{14}$$

when t $_2$is sufficient large, $\left(\frac{2n_i\mu_i V_0}{N_i}\right)t \gg \left(\frac{n_i q\mu_i AR}{\eta_{av}}\right)^2$, so $\left(\frac{n_i q\mu_i AR}{\eta_{av}}\right)^2$ can be omitted. Formula (14) can be reduced to

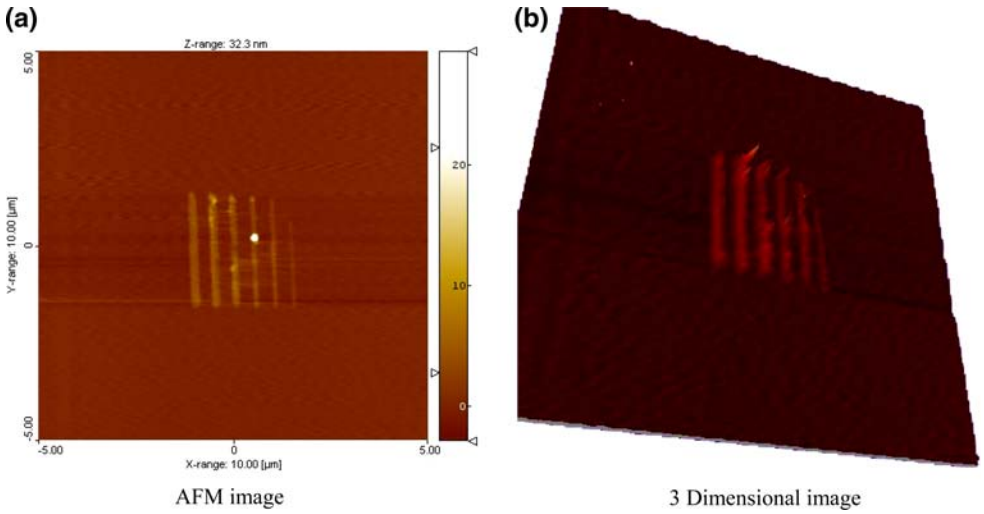

Fig. 3 Al_2O_3 lines fabricated by anodic oxidation (the applied voltage is 20, 18, 16, 14, 12, 10 V from left to right, respectively. Scanning rate is 2.3 μm/s). (**a**) AFM image and (**b**) 3 Dimensional image

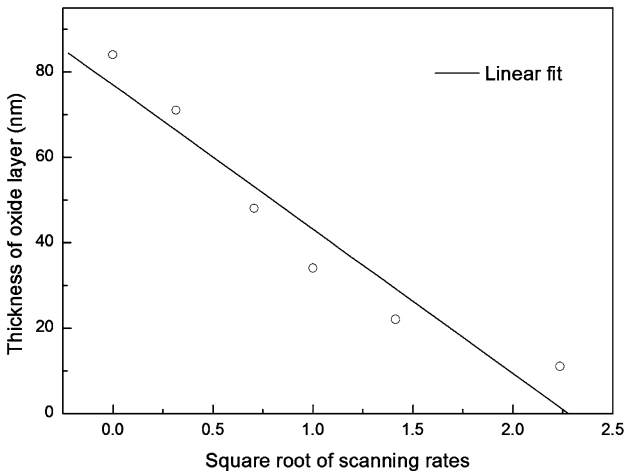

Fig. 5 The relationship between thickness of oxide layer and square root of scanning rate

$$X_0(t) = X_i + \left(\frac{2n_i\mu_i V_0}{N_i}\right)^{1/2} t^{1/2} \quad (15)$$

From the above discussion, we can obtain the conclusion that when the oxidation time is sufficient long (a thicker oxide layer), the thickness of oxide layer is in direct proportion to the square root of applied voltage and oxidation time.

Figure 3 is the AFM image of six parallel Al_2O_3 lines fabricated by AFM anodic oxidation under different applied voltage. It can be observed that the thickness of Al_2O_3 lines varied with the increasing of voltage.

Figure 4 is the AFM image of Al_2O_3 lines fabricated under different scanning rates. From above to bottom the scanning rates were 0.05, 0.1, 0.5, 1, 2 and 5 μm/s, respectively. The applied voltage is 12 V. With slower scanning rate we can get thicker and broader line.

Figure 5 shows the relationship between thickness of oxide layer and square root of scanning rate. From formula (15) we know the thickness is in direct proportion to the square root of oxidation time, which means in inverse proportion to the square root of scanning rate. This conclusion is coinciding with the experiment results in Fig. 5.

4 Conclusions

With AFM fabrication technique, Al_2O_3 nanowire, rings, dot array and pattern were fabricated on Si substrates with SiO_2 surface layer. By analysis the mechanism of anodic oxidation, we find that the thickness of oxide layer is in inverse proportion to the square root of scanning rate. The experimental results proves the conclusion.

Acknowledgements This work was financially supported by MOST 973 Program, grant No. 2006CB705604, Shanghai Leading Academic Disciplines (T0105) and Shanghai Education Committee (Shuguang project), which is gratefully acknowledged.

References

1. J.A. Dagata, J. Schneir, H.H. Harary, C.J. Evans, M.T. Postek, J. Bennett, Appl. Phys. Lett. **56**, 2001 (1990)
2. H. Sugimura, T. Uchida, N. Kitamura, H. Masuhara, J. Vac. Sci. Technol. B **12**, 2884 (1994)
3. K. Matsumoto, S. Takahashi, M. Ishii, M. Hoshi, A. Kurokawa, S. Ichimura, A. Ando, Jpn. J. Appl. Phys. **34**, 1387 (1995)
4. K. Matsuomoto, M. Ishii, K. Segawa, Y. Oka, B.J. Vartanian, J.S. Harris, Appl. Phys. Lett. **68**, 34 (1996)
5. A.E. Gordon, R.T. Fayfield, D.D. Litfin, T.K. Higman, J. Vac. Sci. Technol. B **13**, 2805 (1995)
6. E.S. Snow, P.M. Campbell, Physica B **227**, 279 (1996)
7. R. Held, T. Heinzel, P. Studerus, K. Ensslin, Physica E **27**, 48 (1998)
8. B. Irmer, M. Kehrle, H. Lorenz, J.P. Kotthaus, Semicond. Sci. Technol. **13**, A79 (1998)
9. C. Huh, S.J. Park, J. Vac. Sci. Technol. B **18**, 55 (2000)